Autonomic Nervous System Measurement in Hyperbaric Environments Using ECG and PPG Signals

Alberto Hernando, María Dolores Peláez-Coca, María Teresa Lozano, Montserrat Aiger, David Izquierdo, Alberto Sánchez, María Isabel López-Jurado, Ignacio Moura, Joaquín Fidalgo, Jesús Lázaro, and Eduardo Gil

***Abstract*—The main aim of this paper was to characterize the Autonomic Nervous System response in hyperbaric environments using electrocardiogram (ECG) and pulse-photoplethysmogram (PPG) signals. To that end, 26 subjects were introduced into a hyperbaric chamber and five stages with different atmospheric pressures (1 atm; descent to 3 and 5 atm; ascent to 3 and 1 atm) were recorded. Respiratory information was extracted from the ECG and PPG signals and a combined respiratory rate was studied. This information was also used to analyze Heart Rate Variability (HRV) and Pulse Rate Variability (PRV). The database was cleaned by eliminating those cases where the respiratory rate dropped into the low frequency band (LF: 0.04–0.15 Hz) and those in which there was a discrepancy between the respiratory rates estimated using the ECG and PPG signals. Classical temporal and frequency indices were calculated in such cases. The ECG results showed a time-related dependency, with the heart rate and sympathetic markers (normalized power in LF and LF/HF ratio) decreasing as more time was spent inside the hyperbaric environment. A dependence between the atmospheric pressure and the parasympathetic response, as reflected in the high-frequency band power (HF: 0.15–0.40 Hz), was also found, with power increasing with atmospheric pressure. The combined respiratory rate also reached a maximum in the deepest stage; thus, highlighting a significant difference between this stage and the first one. The PPG data gave similar findings and also allowed the oxygen saturation to be computed; therefore, we propose the use of this signal for future studies in hyperbaric environments.**

***Index Terms*—Autonomic nervous system, ECG, hyperbaric environments, PPG, respiratory rate.**

Manuscript received June 22, 2017; revised November 30, 2017 and January 10, 2018; accepted January 18, 2018. Date of publication January 24, 2018; date of current version January 2, 2019. This work was supported in part by the Ministerio de Economía, Industria y Competitividad, in part by the fondos FEDER through the Project TEC2014-54143-P and TIN2014-53567-R, in part by the Centro Universitario de la Defensa under the Projects CUD2013-11, CUD2016-18, UZCUD2016-TEC-03, and UZCUD2017-TEC-04, in part by DGA T04-FSE, and in part by the European Unions Framework Programme for Research and Innovation Horizon 2020 (2014-2020) under the Marie Skodowska-Curie Grant 745755. *(Corresponding author: Alberto Hernando.)*

A. Hernando and M. D. Peláez-Coca are with the BSICoS Group, Aragón Institute of Engineering Research (I3A), IIS Aragón, University of Zaragoza, Zaragoza 50009, Spain and also with the Centro Universitario de Defensa, Academia General Militar, Zaragoza 50090, Spain (e-mail: alb_her_1991@hotmail.com; mdpelaez@unizar.es).

M. Lozano is with the RoPeRT Group, I3A, University of Zaragoza, Zaragoza 50009, Spain and also with the Centro Universitario de Defensa, Academia General Militar, Zaragoza 50090, Spain (e-mail: maytelo@unizar.es).

M. Aiger, D. Izquierdo, and A. Sánchez are with Centro Universitario de Defensa, Academia General Militar, Zaragoza 50090, Spain (e-mail: montsea@unizar.es; d.izquierdo@unizar.es; asr@unizar.es).

M. I. López-Jurado, I. Moura, and J. Fidalgo are with the Hospital General Militar de la Defensa, Zaragoza 50009, Spain (e-mail: ilopmar@oc.mde.es; jmoubar@et.mde.es; Jfidalgo06@gmail.com).

J. Lázaro is with the Department of Biomedical Engineering, University of Connecticut, Storrs, CT 06269 USA, and also with the BSICoS Group, Aragón Institute of Engineering Research (I3A), IIS Aragón, University of Zaragoza, Zaragoza, Spain (e-mail: jesus.lazaro@esat.kuleuven.be).

E. Gil is with is with the BSICoS Group, Aragón Institute of Engineering Research (I3A), IIS Aragón, University of Zaragoza, Zaragoza, Spain and also with the Centro de Investigación Biomédica en Red Bioingeniería, Biomateriales y Nanomedicina, Madrid, Spain (e-mail: edugilh@unizar.es).

Digital Object Identifier 10.1109/JBHI.2018.2797982

I. Introduction

HUMAN interest in exploring the environment has resulted in several notable achievements, such as air and space travel or undersea exploration. However, as the human body is not adapted to these surroundings, their biological, psychological and physiological effects must be studied. Diving involves prolonged time periods in a hyperbaric environment. However, as water is almost 800 times denser than air, a descent of 10 meters implies a pressure increase of one atmosphere (atm). The maximum descent for recreational diving is fixed at 40 meters, although some professionals, such as scientists or the military, go deeper. Nowadays, approximately 7 million people practice recreational diving [1].

Divers are affected by different factors in the aquatic environment [2], including hydrostatic pressure. According to Poiseuille's law, a decrease in the heart rate is needed to maintain an adequate cardiac output and minimise the effects of hydrostatic pressure [3]. Another factor is the presence of gases inside the body, as the expansion or compression of these gases can cause mechanical alterations. Thus, an increase in the partial pressure of these gases can result in biochemical CO_2, N_2 (narcosis) or O_2 (hyperoxia) intoxication, and they also can form bubbles, thus leading to decompression sickness (DS), with symptoms ranging from minor skin alterations to neurological, cardiopulmonary and inner ear disorders. Furthermore, epidemiological studies have shown an increase in DS and

fatalities in recreational diving over the past few decades [4]. As can be seen, many variables, such as depth, pressure or temperature, affect the body's cardiovascular response during a dive [5].

The fast response to blood pressure changes that occur during a dive is reflected in the Autonomic Nervous System (ANS), which plays a crucial role in the maintenance of homoeostasis and is composed of two branches, namely the sympathetic nervous system and the parasympathetic, or vagal, nervous system. The balance between these branches reflects the efforts of the body to adapt itself to new environments in the best possible manner. Non-invasive techniques can be used to measure ANS activity, with the most common being the Heart Rate Variability signal (HRV), which is extracted from the electrocardiogram (ECG). However, as this technique requires electrodes to be placed at several locations on the subject's chest, it is not the most appropriate method in hyperbaric environments in terms of subject comfort. Another way to measure ANS activity is the Pulse Rate Variability signal (PRV), which is extracted from the pulse-photoplethysmogram (PPG) [6]. Numerous studies carried out at 1 atm suggest that HRV and PRV give the same information about the ANS response [7]–[10], although some controversy still exists [11]. PPG measurement requires only one low-cost device that is widely used in routine clinical practice and can be located on several parts of the body, thus meaning that the PPG signal is better suited to use in such environments. In addition, the PPG signal allows oxygen saturation in the subject to be analysed, which is an additional reason for using PPG to monitor subjects in hyperbaric environments.

Irrespective of the signal used, spectral analysis of HRV or PRV at rest reveals two main components: a low-frequency (LF) component [0.04–0.15 Hz], which reflects both sympathetic and parasympathetic activity, and a high-frequency (HF) component [0.15–0.4 Hz] due to respiratory sinus arrhythmia. In addition, power in the HF band has been used as a measure of parasympathetic activity. Normalised power in the LF band and the ratio between power in LF and HF bands have also been used as a measure of sympathovagal balance [12]. Another interesting signal to be considered in a hyperbaric study is the respiratory one, which can be extracted from ECG or PPG [13]–[19]. In this regard, it has been shown that changes in the respiratory pattern alter the spectral content of HRV [20] and, consequently, the interpretation of sympathetic or vagal activations [21]–[23].

The ANS response has been analysed in multiple studies simulating atmospheric pressure conditions inside a hyperbaric chamber, without needing to go under water [24]–[29]. The results of these studies suggested an increase in the power related to the HF band, thus meaning an increase in parasympathetic activity [24], [26], [27], [29]. Another conclusion from hyperbaric environment studies is a reduction in the heart rate [24], [25], [27], [28], although this trend does not appear in all literature studies [29]. The number of studies analysing ANS during immersion is lower, probably because of the difficulty of obtaining a proper recording in this situation. In real dives, despite the fact that other external uncontrolled variables, such as immersion reflex or cold water stimulus [30], [31] might lead us to presuppose an increase in sympathetic activity, the ANS response shows the same behaviour as inside the hyperbaric chamber: an increase in HF power [32], [33]. This pattern could be explained by a possible rise in baroreceptor sensitivity, with an ensuing increase in parasympathetic activity [34]. All these studies (inside a hyperbaric chamber or under water) are characterised by: a low number of subjects (between 8 and 12), the use of only the HRV to characterise the ANS behaviour, and the measurement of only one hyperbaric stage between 2.5 and 3 atm.

In light of the above, the main goal of this study was to characterise the ANS response to atmospheric pressure changes and the time spent in a hyperbaric environment. To that end, an analysis of HRV, PRV and respiratory rate was performed for 26 healthy subjects inside a hyperbaric chamber during five stages, as determined using the atmospheric pressure recorded. ECG and PPG signals were recorded to study the body's response, thus allowing a comparison of both signals to corroborate that they provide the same information. Respiratory information was extracted from both the ECG and PPG signals, and the resultant estimated respiratory rate was included in the HRV and PRV analysis to obtain a more reliable interpretation of the results. The higher number of subjects in comparison to previous studies, the different stages with varying atmospheric pressures (1 atm; descent to 3 and 5 atm; ascent to 3 and 1 atm), and the analysis and comparison of the ECG and PPG recordings are innovations of this study.

II. Materials

A total of 26 subjects (22 males and 4 females), with a mean age of 28.73 $\pm$ 6.39 years and a strong component of military personnel (21 out of 26, 80.78% of the total study population) were recorded in the study. After receiving approval for the study from the "Comité de ética de la investigación con medicamentos de la inspección general de sanidad de la Defensa" ethics committee, all subjects were recorded inside the hyperbaric chamber of the Hospital General de la Defensa de Zaragoza. The protocol inside the chamber had a duration of about two hours and a schematic representation thereof is shown in Table I. Five different stages involving 5 min stops at 1 atm (sea level), 3 atm (simulating 20 metres depth) and 5 atm (simulating 40 meters depth), and subsequently returning to 3 atm and 1 atm were performed. Most of the time was spent in the decompression stops between 3 atm and 1 atm, as recommended in standard decompression tables. In 21 subjects, this decompression time was 44 min, distributed as follows: 2 min at 1.9 atm, 16 min at 1.6 atm and 26 min at 1.3 atm. In the rest of the cases, this time was slightly fewer, but always upper than 30 min.

Subjects remained relaxed and sitting comfortably, and the chamber was correctly ventilated throughout the protocol in an attempt to avoid major changes in temperature and humidity. Subjects remained in silence and without perform movements during basal stages. The test recorded at 1 and 5 atm measures divided attention, and was not analysed because it is not the main focus of the present study, in which ANS response is characterised in hyperbaric environment. To avoid the influence of the test in the 1 atm basal stage, when it is performed first, only the last 4 min of the basal stage for each simulated depth were used. Therefore, a total of five stages, referred to as B1D,

TABLE I
EXPLANATION OF THE PROTOCOL USED, SHOWING THE ATMOSPHERIC PRESSURE, THE DIFFERENT PARTS AND THEIR RESPECTIVE DURATIONS

Pressure	1 atm (sea level)			1-3 atm	3 atm	3-5 atm	5 atm		5-3 atm	3 atm	3-1 atm	1 atm (sea level)
Explanation	Audio	Test	Basal	Descending	Basal	Descending	Basal	Test	Ascending	Basal	Ascending	Basal
Duration	5 min	7-8 min	5 min	6-8 min	5 min	6-8 min	5 min	7-8 min	6-8 min	5 min	50-55 min	5 min

B3D, B5, B3A and B1A (B from basal; the number reflects the pressure, n atm; the letter D or A refers to descent or ascent) were studied to see if there were any physiological differences between them.

Recordings were performed using a Nautilus device [35], which allows the ECG signal to be recorded with three leads at a sampling frequency (fs) of 2000 Hz, along with the PPG signal (fs = 1000 Hz) on the finger at two possible wavelengths (red and infra-red) and the atmospheric pressure (fs = 250 Hz) inside the chamber.

III. METHODS

A. Extraction of ECG and PPG Information

ECG and PPG signals need some pre-processing before analysis. Thus, ECG is first down-sampled to 1000 Hz to obtain the same sampling frequency as for the PPG signal. A low-pass FIR filter is then applied to the two signals to estimate the baseline interference and to remove this noise from the signal (cut-off frequency of 0.03 Hz and 0.07 Hz for ECG and PPG signals respectively) [36]. Another low-pass FIR filter is applied over the PPG signal (cut-off frequency of 35 Hz) to remove the high frequency noise [18].

Heart beats are detected in the ECG using a wavelet-based algorithm over the frontal bipolar second lead of the recorded ECG signal [37]. This is an accurate and robust method for detecting characteristic wave peaks and boundaries in the ECG using a single analysis stage, namely dyadic wavelet transform of the ECG signal. In addition, ectopic beats and missed and false detections are identified and corrected [38]. As a result, the QRS complex can be located in the ECG, and the difference between consecutive R waves is used to generate the RR time series.

Artefactual pulses in the PPG signal ($x_{\mathrm{PPG}}(n)$) were suppressed using the artefact detector described in [39]. The apex (n_{Ai}), basal (n_{Bi}) and medium points (n_{Mi}) of the PPG pulses were then detected automatically using an algorithm based on a low-pass differentiator filter [40]. Fig. 1 shows a PPG signal in which more representative points are highlighted. As the medium points are considered the fiducial points in PPG because of their robustness [41], they are used to compute the pulse-to-pulse (PP_{i}) time series as the difference between consecutive n_{Mi}.

Both analysis are similar from this point on. The time-varying integral pulse frequency modulation model (TVIPFM) is used to determine the influence of the ANS on the beat/pulse occurrence time series [42]. This model compensates the influence of the mean heart rate over the modulating signal, thus providing more realistic ANS activity information. The instantaneous heart/pulse rate signal ($d_{\mathrm{XR}}(n)$ with $\mathrm{X} \in [\mathrm{H}, \mathrm{P}]$), sampled at 4 Hz, is represented by:

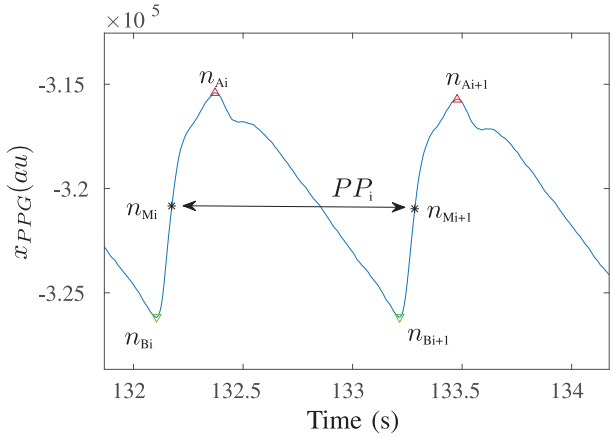

Fig. 1. Two pulse waves in the PPG signal (in arbitrary units, au) with their most representative points highlighted: apex (n_{Ai} and $n_{\mathrm{Ai+1}}$), basal (n_{Bi} and $n_{\mathrm{Bi+1}}$) and medium points (n_{Mi} and $n_{\mathrm{Mi+1}}$). The distance between two adjacent mid-points is the pulse-to pulse-interval or PP_{i}, which is used to compute the time series.

$$d_{\mathrm{XR}}(n) = \frac{1 + \mathfrak{m}_{\mathrm{X}}(n)}{T_{\mathrm{X}}(n)}, \tag{1}$$

where $\mathfrak{m}_{\mathrm{X}}(n)$ represents the modulating signal that carries the information from ANS and $T_{\mathrm{X}}(n)$ is the time-varying mean heart/pulse period.

Assuming that the variations in the term $\frac{1}{T_{\mathrm{X}}(n)}$ are slower than those in the term $\frac{\mathfrak{m}_{\mathrm{X}}(n)}{T_{\mathrm{X}}(n)}$ the time-varying mean HR or PR, ($d_{\mathrm{XRM}}(n)$), can be obtained by low-pass filtering $d_{\mathrm{XR}}(n)$, with a cut-off frequency of 0.03 Hz, as follows:

$$d_{\mathrm{XRM}}(n) = \frac{1}{T_{\mathrm{X}}(n)}. \tag{2}$$

HRV and PRV signals ($d_{\mathrm{XRV}}(n)$) are subsequently obtained as:

$$d_{\mathrm{XRV}}(n) = d_{\mathrm{XR}}(n) - d_{\mathrm{XRM}}(n) = \frac{\mathfrak{m}_{\mathrm{X}}(n)}{T_{\mathrm{X}}(n)}. \tag{3}$$

Finally, $\mathfrak{m}_{\mathrm{X}}(n)$ is estimated by correcting $d_{\mathrm{XRV}}(n)$ by $d_{\mathrm{XRM}}(n)$:

$$\mathfrak{m}_{\mathrm{X}}(n) = \frac{d_{\mathrm{XRV}}(n)}{d_{\mathrm{XRM}}(n)}. \tag{4}$$

Fig. 2 shows $d_{\mathrm{XR}}(n)$, $d_{\mathrm{XRM}}(n)$, and $\mathfrak{m}_{\mathrm{X}}(n)$ signals extracted from the ECG (upper image) and from the PPG (lower image). Paired signals are very similar and contain the same information.

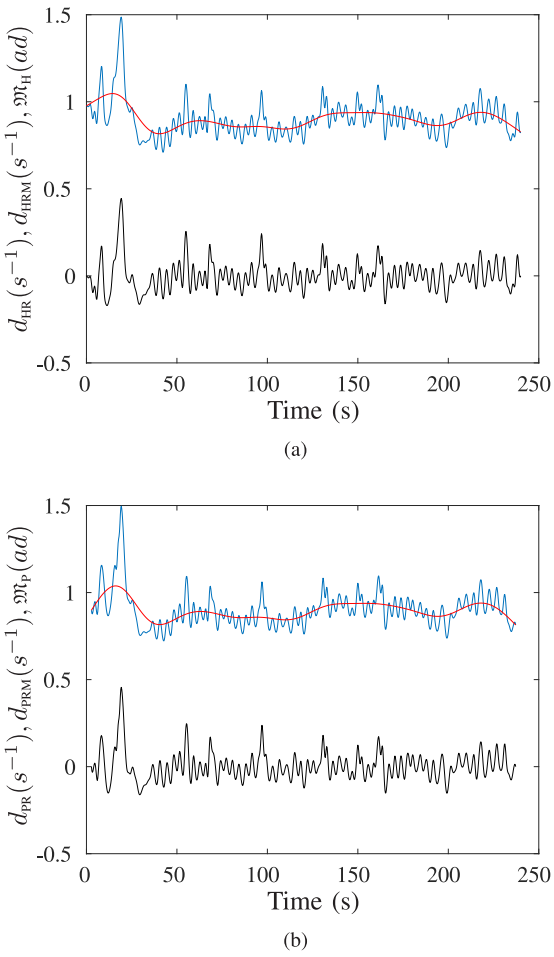

Fig. 2. $d_{\mathrm{XR}}(n)$ (in blue), $d_{\mathrm{XRM}}(n)$ (in red) and $\mathfrak{m}_{\mathrm{X}}(n)$ (in black) extracted from the ECG (a) and from the PPG (b).

Four temporal parameters can be computed for both signals using the beat-to-beat/pulse-to-pulse time series:

- $NN(s)$: median of the Normal-to-Normal intervals between the fiducial points of both signals.
- $IQR(s)$: Interquartile range as a measure of statistical dispersion, which reflects the difference between the upper and lower quartiles.
- $RMSSD(s)$: square root of the mean of the squares of the successive differences between adjacent NN intervals.
- $pNN50(\%)$: number of pairs of successive NNs that differ by more than 50 ms, divided by the total number of NN intervals.

Four frequency parameters were calculated based on the power spectral distribution (PSD) analysis of the modulating signal $\mathfrak{m}_{\mathrm{X}}(n)$. The 4-min-duration recorded for every atmospheric pressure stage was considered stationary given the repose state maintained in these periods, which does not change rapidly. Therefore, classic frequency domain indices were computed for the $\mathfrak{m}_{\mathrm{X}}(n)$ signal using Welch's power spectral density estimation, with seven 1-min Hamming windows and an overlap of 50%. The parameters computed are:

- $P_{\mathrm{LF}}(ad)$: power inside the LF band (0.04–0.15 Hz). Measurement units: ad, adimensional units.
- $P_{\mathrm{HF}}(ad)$: power inside the HF band (0.15–0.4 Hz).
- $P_{\mathrm{LF_n}}(nu)$: power in LF band normalised with respect to those of the LF and HF bands. Measurement units: nu, normalised units.
- $R_{\mathrm{LF/HF}}(nu)$: ratio between LF and HF power.

These eight parameters allow the response of the ANS to atmospheric pressure changes and time spent in the hyperbaric chamber to be characterised. Furthermore, the fact that parameter extraction is performed using the $\mathfrak{m}_{\mathrm{H}}(n)$ and $\mathfrak{m}_{\mathrm{P}}(n)$ signals allows a comparison between ECG and PPG estimations to be made in order to determine whether both signals also provide the same information in hyperbaric environments.

B. Respiratory Information Extracted From ECG and PPG

Respiratory information completes the ANS analysis. The vagal tone reflects respiratory sinus arrhythmia (RSA), which is synchronous with respiration; therefore the relationship between respiratory rate and the parasympathetic system must be taken into consideration during the analysis. Those subjects with a respiratory rate lower than 0.15 Hz (upper limit of the LF band) were discarded to avoid possible misinterpretations when studying the ANS results [23].

Respiratory information can be extracted from the ECG and PPG. In order to increase the robustness of the method, the first step involved obtaining all the derived respiration signals for the ECG (EDR) and the PPG (PDR). Secondly, and after combining the EDR and PDR signals, the same algorithm was applied to them to obtain the respiratory rate. Finally, a combined respiratory rate was averaged if both estimations provided a similar value during at least one minute of the analysis window. If not, no respiratory rate estimation was performed for that subject at that stage.

The method for estimating respiratory rate from ECG presented in [16] was used. This method exploits respiration-induced morphology variations in the ECG signal based on three signals, namely the R-wave angle, upwards to the R wave slope and downwards to the R wave slope [43]. The method assigns the value of its associated R-wave angle or QRS slope to each beat detected. As these signals are unevenly sampled, a resampling at 4 Hz is necessary to standardise them. Finally, a mad-based-outlier rejection and a band-pass filter (0.075–1 Hz cut-off frequencies, to study only the frequency range where the respiratory rate is expected to be found [19]) were applied. Three leads are registered in this study, with three EDR signals estimated for each lead, thus meaning that nine final EDR signals are used in the ensemble to extract respiratory information.

The algorithm explained in [18] was applied to estimate respiratory information from the PPG. In addition to the PRV signal extracted, two morphology-based PDR signals, namely the Pulse Amplitude Variability (PAV), which reflects the amplitude variation between the apex and the basal points, and the Pulse Width Variability (PWV), were also estimated. As both signals are unevenly sampled, a resampling at 4 Hz was applied to standardise them, along with a mad-based-outlier rejection and a band-pass filter (0.075-1 Hz cut-off frequencies). These

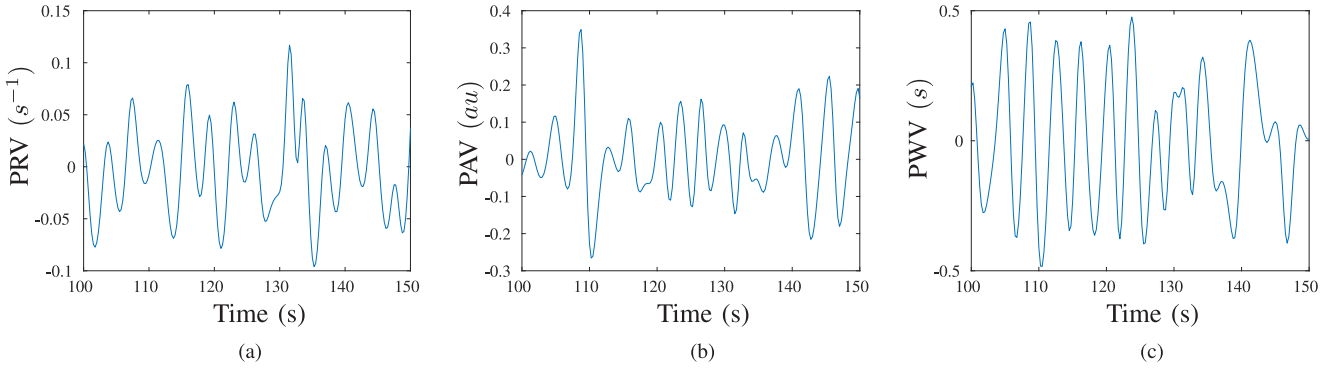

Fig. 3. 50 seconds of the 3 PDR signals affected by respiration: (a) PRV; (b) PAV; (c) PWV.

two signals, and the PRV obtained previously, make up the ensemble used to extract respiratory information from the PPG. An example of these three PDR signals is shown in Fig. 3.

A fusion technique based on [16] was applied to the nine EDR signals (j = 1...9) and the three PDR signals (j = 1...3) to estimate respiratory frequency ($F_{\mathrm{R}}^{\mathrm{X}}$) from "peaked-conditioned" averaged spectra. The same algorithm was applied to both signals. Despite this, a minor modification in the estimated respiratory rate is necessary when PPG signals are used given the fact that the low frequency components are not related to respiration, as they are responsible for the changes in the peakness conditions and limits, as discussed in [15].

A power spectrum density $S_{\mathrm{j,k}}^{\mathrm{X}}(f)$ was estimated every 5 seconds from the k^{th} 40 s length running window using the Welch's periodogram with sub-windows of 12 s and a 50% overlap, for both cases (X) and for each DR signal (j). The location of the largest peak $f_{\mathrm{I}}^{\mathrm{X}}(j,k)$ was determined for each $S_{\mathrm{j,k}}^{\mathrm{X}}(f)$. A reference interval $\Omega_{\mathrm{R}}^{\mathrm{X}}(j,k)$ was subsequently established as:

$$\Omega_{\mathrm{R}}^{\mathrm{X}}(j,k) = \left[F_{\mathrm{R}}^{\mathrm{X}}(j,k-1) - \delta, F_{\mathrm{R}}^{\mathrm{X}}(j,k-1) + 2\delta\right], \quad (5)$$

where $F_{\mathrm{R}}^{\mathrm{X}}(k-1)$ is the respiratory frequency estimated from the previous $(k-1)$ window, and $\delta = 0.1$. All peaks larger than 85% of $f_{\mathrm{I}}^{\mathrm{X}}(j,k)$ inside $\Omega_{\mathrm{R}}^{\mathrm{X}}(j,k)$ were detected, and $f_{\mathrm{II}}^{\mathrm{X}}(j,k)$ was chosen as the nearest peak to $F_{\mathrm{R}}^{\mathrm{X}}(j,k-1)$. Note that $f_{\mathrm{II}}^{\mathrm{X}}(j,k)$ can be the same $f_{\mathrm{I}}^{\mathrm{X}}(j,k)$ if the largest peak is also the nearest peak to $F_{\mathrm{R}}^{\mathrm{X}}(j,k-1)$.

A measure of peakness was subsequently obtained from $S_{\mathrm{j,k}}^{\mathrm{X}}(f)$ as the percentage of power around the $f_{\mathrm{II}}^{\mathrm{X}}(j,k)$ with respect to the reference interval $\Omega_{\mathrm{R}}^{\mathrm{X}}(j,k)$. The peakness is determined from ECG signal as:

$$P_{\mathrm{j,k}}^{\mathrm{H}} = \frac{\int_{f_{\mathrm{II}}^{\mathrm{H}}(j,k)-0.6\delta}^{f_{\mathrm{II}}^{\mathrm{H}}(j,k)+0.6\delta} S_{\mathrm{j,k}}^{\mathrm{H}}(f)df}{\int_{F_{\mathrm{R}}^{\mathrm{H}}(k-1)-\delta}^{F_{\mathrm{R}}^{\mathrm{H}}(k-1)+2\delta} S_{\mathrm{j,k}}^{\mathrm{H}}(f)df} \times 100, \quad (6)$$

A different peakness formulation, which uses the criterion described in [15] to enhance the high frequencies in the PPG algorithm, is used for the PPG:

$$P_{\mathrm{j,k}}^{\mathrm{P}} = \frac{\int_{(1-g)\cdot f_{\mathrm{II}}^{\mathrm{P}}(j,k)}^{(1+g)\cdot f_{\mathrm{II}}^{\mathrm{P}}(j,k)} S_{\mathrm{j,k}}^{\mathrm{P}}(f)df}{\int_{F_{\mathrm{R}}^{\mathrm{P}}(k-1)-\delta_{\mathrm{P}}}^{F_{\mathrm{R}}^{\mathrm{P}}(k-1)+\delta_{\mathrm{P}}} S_{\mathrm{j,k}}^{\mathrm{P}}(f)df} \times 100, \quad (7)$$

where $g = 0.5$ and $\delta_{\mathrm{P}} = 0.2$. This is the only difference between ECG and PPG respiratory rate estimations.

A peaked-conditioned average spectra, $\bar{S}_{\mathrm{k}}^{\mathrm{X}}(f)$, was then obtained by averaging those $S_{\mathrm{j,k}}^{\mathrm{X}}(f)$ which are sufficiently peaked:

$$\bar{S}_{\mathrm{k}}^{\mathrm{X}}(f) = \sum_{l=-L_s}^{L_s} \sum_{j=1}^{N_s} \chi_{\mathrm{j,k\text{-}l}}^{\mathrm{A}} \chi_{\mathrm{j,k\text{-}l}}^{\mathrm{B}} S_{\mathrm{j,k\text{-}l}}^{\mathrm{X}}(f), \quad (8)$$

where L_s was set to 2 in order to average a maximum of 5 spectra for each DR signal as in [16], N_s is the number of signals (9 for ECG and 3 for PPG), and $\chi_{\mathrm{j,k\text{-}l}}^{\mathrm{A}}$ and $\chi_{\mathrm{j,k\text{-}l}}^{\mathrm{B}}$ are two criteria used to determine whether the power spectrum $S_{\mathrm{j,k\text{-}l}}^{\mathrm{X}}(f)$ is sufficiently peaked:

$$\chi_{\mathrm{j,k}}^{\mathrm{A}} = \begin{cases} 1, & P_{\mathrm{j,k}}^{\mathrm{X}} \geq 85 \\ 0, & \text{otherwise} \end{cases}, \quad (9)$$

$$\chi_{\mathrm{j,k}}^{\mathrm{B}} = \begin{cases} 1, & P_{\mathrm{j,k}}^{\mathrm{X}} \geq \max_j\left(P_{\mathrm{j,k}}^{\mathrm{X}}\right) - \lambda \\ 0, & \text{otherwise} \end{cases}, \quad (10)$$

with only those $S_{\mathrm{j,k}}^{\mathrm{X}}(f)$ whose $P_{\mathrm{j,k}}^{\mathrm{X}}$ was above 85% and had a total power close to the maximum ($\lambda = 0.05$) being averaged. Fig. 4 displays two spectra as examples, one with $P_{\mathrm{j,k}}^{\mathrm{X}} > 85\%$ (sufficiently peaked to be used for the average), and another one with $P_{\mathrm{j,k}}^{\mathrm{X}} < 85\%$ (insufficiently peaked to be used for the average).

Consequently, the respiratory rate is estimated for both signals as the maximum of $\bar{S}_{\mathrm{k}}^{\mathrm{X}}(f)$:

$$F_{\mathrm{R}}^{\mathrm{X}}(k) = \arg\max_f \bar{S}_{\mathrm{k}}^{\mathrm{X}}(f). \quad (11)$$

Finally, a combined respiratory rate ($F_{\mathrm{R}}^{\mathrm{C}}(k)$) was calculated as the mean of both estimations if they are similar. The difference between PPG and ECG values must be less than 0.05 Hz for at least 25% of the analysis window. This restriction was defined based on the estimation errors found in [16], [18], and imposes

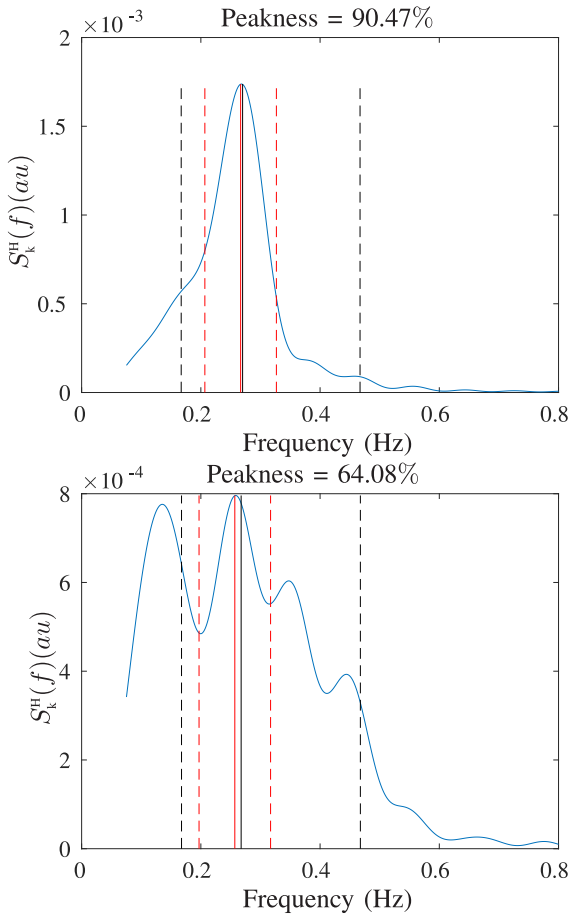

Fig. 4. Differences between spectra that satisfy the peakness condition and spectra that do not. Red lines illustrate the limits of the integrating interval of the numerator in $P_{j,k}^{H}$ with the solid line marking the $f_{II}^{H}(k)$ value. Black dashed lines illustrate the reference interval $\Omega_{R}^{H}(k)$, with the solid line representing the previous estimated respiratory rate $F_{R}^{H}(k-1)$.

that, to obtain the mean respiratory rate value representing the entire stage ($\overline{F}_{R}^{C}$), both estimations have to be similar for at least during 1 min. If this criterion is not fulfilled, the combined respiratory rate is not estimated in that subject for that stage.

The percentage of time (P_T) during which both estimations matched was also calculated:

$$P_T(\%) = \frac{100}{N_t} \times \sum_{k=0}^{T_n} C_f(k), \tag{12}$$

where $C_f(k) = 1$ if both estimations match and $C_f(k) = 0$ if not, and N_t is the total number of time instants.

C. Statistical Analysis

Two different statistical tests were used to analyse the use of PRV as a surrogate for HRV. The first of these was a comparison between ECG and PPG likeness by means of the correlation of the modulating signal $\mathfrak{m}_X(n)$ extracted from the ECG and from the PPG. The second one involved an analysis of the difference for each parameter extracted from HRV and PRV, with a Shapiro-Wilk test being applied to verify the normal distribution of the eight parameters and then a paired sample Student's t-test being applied to the same parameter extracted with both signals. The correlation between the parameters extracted was also studied as a marker for the similarity between the two signals.

A further statistical analysis was applied to each parameter to determine the presence of significant differences between the five stages of the protocol. Thus, a Shapiro-Wilk test was applied to check the normal distribution of the parameter, with Student's t-test being applied to every pair of stages if the distribution was normal and the Wilcoxon paired test if not. In both methods, a p-value < 0.05 indicated statistical significance. The aim of this study was to evaluate if the variation in atmospheric pressure or the fact of being in the hyperbaric chamber for a prolonged time modified the physiological parameters.

D. Oxygen Saturation

Oxygen saturation can be computed using both wavelengths (red and infra-red) of the PPG signal, applying the decomposition in alternating and direct components (AC and DC) [44]. Both signals were initially band-pass-filtered with cut-off frequencies of 0.4 and 10 Hz. They were then divided into series of 0.8 s and the maximum and minimum determined for each series. The AC component in the red and infra-red wavelengths was described as the difference between the maximum and minimum values, whereas the DC component is just the maximum value. This allowed two ratios, namely the red ratio, which is obtained by dividing the AC component by the DC component, and the infra-red ratio, which is the same operation but for the infra-red wavelength, to be defined. The division of these two ratios gives the so-called ratio of ratios ($R(n)$). Finally, the oxygen saturation $SpO_2(\%)$ was calculated (and expressed as a percentage) according to the device manufacturer's instructions. The oxygen saturation equation was extracted from an experimental calibration curve obtained by comparing this device's recordings with a reference device to obtain the same oxygen saturation measures:

$$SpO_2(\%) = \left[-4.73R(n)^2 + 1.12R(n) + 99.7\right] \times 100. \tag{13}$$

IV. Results

In the following Sections, data for one subject is only available for stages B1D, B3D and B5 as the recording suddenly stopped, thus meaning that the final two stages could not be recorded. As such, there are 26 subjects for B1D, B3D and B5 and 25 subjects for B3A and B1A. As the results obtained for the red and infra-red wavelengths in the PPG signal are very similar, only those for the red configuration are shown to help the reader's understanding.

A. Respiratory Parameters

As mentioned above, two ways to estimate the respiratory rate, one involving the ECG signal and the other the PPG signal, have been proposed. When both estimations are very close for at least one minute during the stage, a mean combined respiratory rate $\overline{F}_{R}^{C}$ can be computed. As this requirement is not always fulfilled, the number of final subjects in each stage varies. The mean and standard deviation (SD) for the combined respiratory

TABLE II
MEAN AND SD FOR THE COMBINED RESPIRATORY RATE ESTIMATION $\overline{F_R^C}$ AND THE PERCENTAGE OF TIME WHEN BOTH ESTIMATIONS MATCH $\overline{P_T}$

Stages	B1D	B3D	B5	B3A	B1A
Subjects	22	20	19	22	21
$\overline{F_R^C}(Hz)$	0.21 ± 0.07	0.23 ± 0.06	0.25 ± 0.05 ⋆	0.26 ± 0.06 ⋆	0.24 ± 0.07
$\overline{P_T}(\%)$	81.29 ± 18.75	78.08 ± 18.67	75.68 ± 20.53	83.06 ± 16.29	81.17 ± 15.84

Statistical differences ($p < 0.05$) are represented by a ⋆ when compared with B1D.

rate and percentage of time that both estimations have a similar value for each stage are presented in Table II.

As the normal distribution was verified, a paired Student's t-test was performed to detect any differences in respiratory rate by stage. The number of subjects studied in the complete database comparisons are: 15 for B3A vs. B3D; 16 for B3A vs. B1D, B5 vs. B3D, B1A vs. B3D, B3A vs. B5 and B1A vs. B5; 17 for B5 vs. B1D and B1A vs. B1D; 18 for B3D vs. B1D; and 20 for B1A vs. B3A. Only significant differences with respect to B1D has been found.

The overall results show that the respiratory rate is higher in the latter stages than in the initial ones, with a significant difference being found when comparing B5 and B3A with B1D. The percentage of time with a match between both estimations ($\overline{P_T}(\%)$) decreased as the atmospheric pressure increased, although the difference was not significant. It must be noted that three subjects in B1D, and one subject in B3D, B5, B3A and B1A, had a respiratory rate value lower than 0.15 Hz, thus meaning that they were discarded in the ANS interpretation.

B. HRV and PRV Parameters

As mentioned above, interpretation of the ANS depends on the respiration. As such, those subjects for whom both estimations did not match or with a respiratory rate lower than 0.15 Hz were discarded. The inter-subject mean and SD for the eight parameters in every stage for the ECG and PPG signals (HRV and PRV), the p-value (T-TEST (p)) and the correlation (CORR) for both signals are presented in Table III. Fig. 5 shows one boxplot for each parameter to highlight the similarity between the ECG and PPG and the trend for each parameter during the various stages. In these boxplots, and in a similar manner to the respiratory rate, a paired statistical test comparing the different stages is carried out, with different numbers of subjects involved in the comparison depending on the stages analysed: 15 subjects for B5 vs. B3D, B1A vs. B3D and B1A vs. B5; 18 for B1A vs. B3A; and 14 for the remaining comparisons.

The similarity between HRV and PRV is demonstrated by the correlation between the signals and the parameters extracted from them. The median value for the correlation between the modulating signals from the ECG and PPG is higher than 95% for all stages. Moreover, the temporal and frequency parameters extracted from them are also essentially identical: both distributions are similar ($p > 0.05$) for all the parameters during all stages and the correlation is higher than 90% in almost all cases (see Table III).

As regards the trend in each temporal parameter, NN and $RMSSD$ increase in value with each stage, whereas IQR and $pNN50$ reach a maximum at stage B5. The statistical analysis showed that all stages are significantly different from the first one in terms of all four parameters. The last two stages (B3A and B1A) also present statistically significant differences with the previous two stages (B3D and B5) for NN and $RMSSD$. However, $pNN50$ has a different distribution, with significant differences being found for B5 vs. B3D and B3A vs. B3D.

With regard to the frequency parameters, P_{HF} exhibits the main difference, being higher in the PPG signal than in the ECG signal, thus affecting the normalised power and the ratio. As for the trend in each frequency parameter, P_{LF} and P_{HF} increase during the descent, reaching a maximum at the deepest stage B5 and then decreasing in value during the ascent. Significant differences were found in P_{LF} when comparing B3A and B1A with B3D and B5, and B5 is significantly different from B1D, but only when P_{LF} is extracted from the PPG signal. P_{HF} is significantly higher in B5 than B1D, and B1A exhibits a significant difference with respect to B5, but only in the PPG signal. In general terms, P_{LF_n} and $R_{LF/HF}$ are higher during the initial stages and their values decrease continuously in the latter stages. Significant differences were found for B5 vs. B1D, B3A vs. B1D and B3A vs. B3D in both markers of sympathetic dominance.

C. Oxygen Saturation

The mean of the $SpO_2(n)$ was computed for each subject in each stage. Table IV shows the inter-subject mean of $SpO_2(\%)$ for each stage. As can be seen, oxygen saturation remains stable during all the stages.

V. DISCUSSION

ECG and PPG signals have been recorded for subjects inside a hyperbaric chamber when simulating different atmospheric pressures, subsequently analysing the five stages proposed. The main goal of this study was to characterise the ANS response to pressure changes and the time spent in the hyperbaric environment. To that end, an analysis of HRV and PRV temporal and frequency parameters was performed. A comparison of the HRV-PRV results was also carried out to corroborate that both signals provide the same information and in order to be able to subsequently use only the most suitable PPG for future studies in these environments. Respiratory information was extracted from both signals and included in the HRV and PRV analysis in order to complete the study of the ANS response to these simulated pressures.

The main limitation of this work is the lack of a respiratory rate reference. To minimise the likely effect, two validated algorithms were implemented to extract respiratory information from the ECG and PPG signals in order to guide the HRV and PRV analysis. As the main goal of this study was to characterise the ANS in hyperbaric environments, a "conservative" criterion was adopted, thereby maximising the robustness of the estimation by merging the respiratory information from the ECG and PPG. A similarity criterion was also imposed in order to increase the robustness of the respiratory rate estimation and attempt to minimise the limitation resulting from this

TABLE III
MEAN ± SD FOR TEMPORAL AND FREQUENCY PARAMETERS IN EACH STAGE FOR ECG AND PPG SIGNAL, ALONG WITH P-VALUE AND CORRELATION FOR BOTH SIGNALS

Stage	Subjects	Parameters	$\overline{NN}(s)$	$\overline{IQR}(s)$	$\overline{RMSSD}(s)$	$\overline{pNN50}(\%)$	$\overline{P_{\mathrm{LF}}}(ad)$	$\overline{P_{\mathrm{HF}}}(ad)$	$\overline{P_{\mathrm{LF_n}}}(nu)$	$\overline{R_{\mathrm{LF/HF}}}(nu)$
B1D	19	HRV	0.92 ± 0.14	0.08 ± 0.03	0.92 ± 0.14	11.96 ± 10.02	2.90 ± 1.56	1.44 ± 0.98	0.67 ± 0.12	2.67 ± 1.78
		PRV	0.92 ± 0.15	0.09 ± 0.03	0.93 ± 0.13	13.58 ± 10.21	2.88 ± 1.46	1.58 ± 1.03	0.66 ± 0.13	2.49 ± 1.75
		T-TEST (p)	0.99	0.77	0.86	0.64	0.98	0.69	0.54	0.78
		CORR	0.99	0.99	0.94	0.99	0.96	0.98	0.89	0.90
B3D	19	HRV	0.99 ± 0.18	0.11 ± 0.05	1.01 ± 0.18	16.58 ± 11.99	3.53 ± 2.42	1.37 ± 0.81	0.66 ± 0.18	3.31 ± 2.58
		PRV	0.99 ± 0.18	0.12 ± 0.05	0.99 ± 0.17	19.21 ± 11.74	3.79 ± 2.63	1.60 ± 0.87	0.65 ± 0.17	2.76 ± 1.71
		T-TEST (p)	0.97	0.60	0.78	0.52	0.79	0.48	0.90	0.49
		CORR	0.99	0.99	0.99	0.96	0.99	0.87	0.96	0.88
B5	18	HRV	1.00 ± 0.17	0.13 ± 0.08	1.01 ± 0.16	21.99 ± 13.75	3.77 ± 3.09	2.44 ± 2.30	0.60 ± 0.18	2.26 ± 2.04
		PRV	0.99 ± 0.17	0.15 ± 0.08	0.99 ± 0.17	24.43 ± 13.03	3.84 ± 3.30	2.71 ± 2.45	0.58 ± 0.18	2.05 ± 1.69
		T-TEST (p)	0.99	0.55	0.74	0.65	0.95	0.75	0.77	0.76
		CORR	0.99	0.88	0.98	0.98	0.99	0.99	0.99	0.98
B3A	21	HRV	1.06 ± 0.19	0.11 ± 0.06	1.06 ± 0.19	18.74 ± 11.84	2.38 ± 2.01	1.37 ± 0.96	0.59 ± 0.15	1.98 ± 1.52
		PRV	1.05 ± 0.19	0.12 ± 0.05	1.05 ± 0.18	21.43 ± 11.58	2.34 ± 1.98	1.57 ± 1.04	0.57 ± 0.14	1.60 ± 0.84
		T-TEST (p)	0.97	0.75	0.90	0.47	0.90	0.60	0.55	0.40
		CORR	0.99	0.99	0.99	0.98	0.97	0.98	0.92	0.87
B1A	20	HRV	1.07 ± 0.19	0.13 ± 0.07	1.08 ± 0.20	19.38 ± 11.07	2.42 ± 2.08	1.64 ± 1.34	0.58 ± 0.18	2.04 ± 1.55
		PRV	1.07 ± 0.19	0.14 ± 0.09	1.07 ± 0.18	20.92 ± 10.51	2.64 ± 2.31	1.68 ± 1.27	0.58 ± 0.18	2.03 ± 1.48
		T-TEST (p)	0.96	0.58	0.87	0.65	0.75	0.98	0.99	0.99
		CORR	0.99	0.88	0.95	0.97	0.96	0.98	0.94	0.94

The number of subjects is also indicated for each stage.

TABLE IV
MEAN ± SD FOR THE PERCENTAGE OF OXYGEN SATURATION DURING EACH STAGE

Stages	B1D	B3D	B5	B3A	B1A
$\overline{SpO_2}(\%)$	96.16 ± 0.10	96.12 ± 0.08	96.15 ± 0.08	96.13 ± 0.06	96.18 ± 0.09

lack of respiratory reference. It should be noted that the two algorithms used [16], [18] were tested with respect to a reference device and the good results obtained validate their use for estimating respiratory rates. In addition, the possibility of both algorithms providing the same wrong result at the same time is considered highly unlikely in this work as they are based on different physiological principles. The threshold of the similarity criterion is based on the margin of error reported for the EDR [16] and PDR [18] methods. In the worst case, the error has an SD of approximately 0.025 Hz, therefore this value was doubled (0.05 Hz) to provide the threshold of likeness. In addition, the similarity must be maintained for at least 1 min of each 4 min stage (25%) in order to correctly characterise the respiratory rate for the stage as a whole.

As no bibliography information could be found concerning respiratory rates in a hyperbaric environment, novel important results are provided in this paper. The general trend is an increase in respiratory rate as the simulated depth increases, with a lower value at 1 atm than at 3 atm and a maximum for stage B5. The fact that almost the same result was obtained for B5 and B3A can be explained by considering that these two stages are very close in time and therefore there may not have been sufficient time to recover normal breathing. These similar measurements explain the fact that differences in the complete database are significant when comparing B5 and B3A with respect to B1D.

No statistically significant differences between stages were found when considering the percentage of time when the difference between the two estimations was less than the established threshold (P_{T}). However, an increase in the mismatch between the two respiratory rates when the pressure increased could be distinguished. One possible explanation for this pattern may be a change in the PPG waveform morphology as a result of the pressure variations. This change may lead to differences in the respiratory signals derived from this PPG, which in turn could affect the respiratory rate estimation. Another possible explanation for the mismatch between respiratory rates, especially as high pressures are reached, could be that respiratory modulation in the ECG and PPG does not behave the same in all cases. As this varies depending on various factors and between subjects [19], it is possible that the different physiological factors affecting respiratory modulation are influenced by pressure changes in a different way. On the one hand, the ECG-based method exploits the morphological changes in QRS complexes provoked by the movement of the electrodes with respect to the heart, and to the impedance changes in the thorax. In contrast, the PPG-based method exploits ANS control over the cardiovascular system and intrathoracic pressure changes. This therefore means that respiratory information is sometimes very clear in the modulating signals whereas sometimes it is not, thus increasing the results variability. Furthermore, as the peakness criteria in this work are very strict, if the respiratory component is not very clear, the algorithm uses the previous estimated respiratory rate and does not update it. If this behaviour is repeated for a long period of time with ECG or PPG signals, and new estimations are calculated in the other one, it is possible that the final results do not match, thereby increasing the time during which the two estimations do not match and its variability.

The limitation of a lack of respiratory signal was minimised by using different respiratory rate estimation techniques from the literature based on different physiological principles. If these techniques provided similar results, respiration was assumed to have been correctly measured. In this study, more importance was given to having a clear respiratory component than to having more time during which the respiratory rate can be estimated, with the final aim of correctly characterising the ANS response to pressure changes using realistic respiratory rate information.

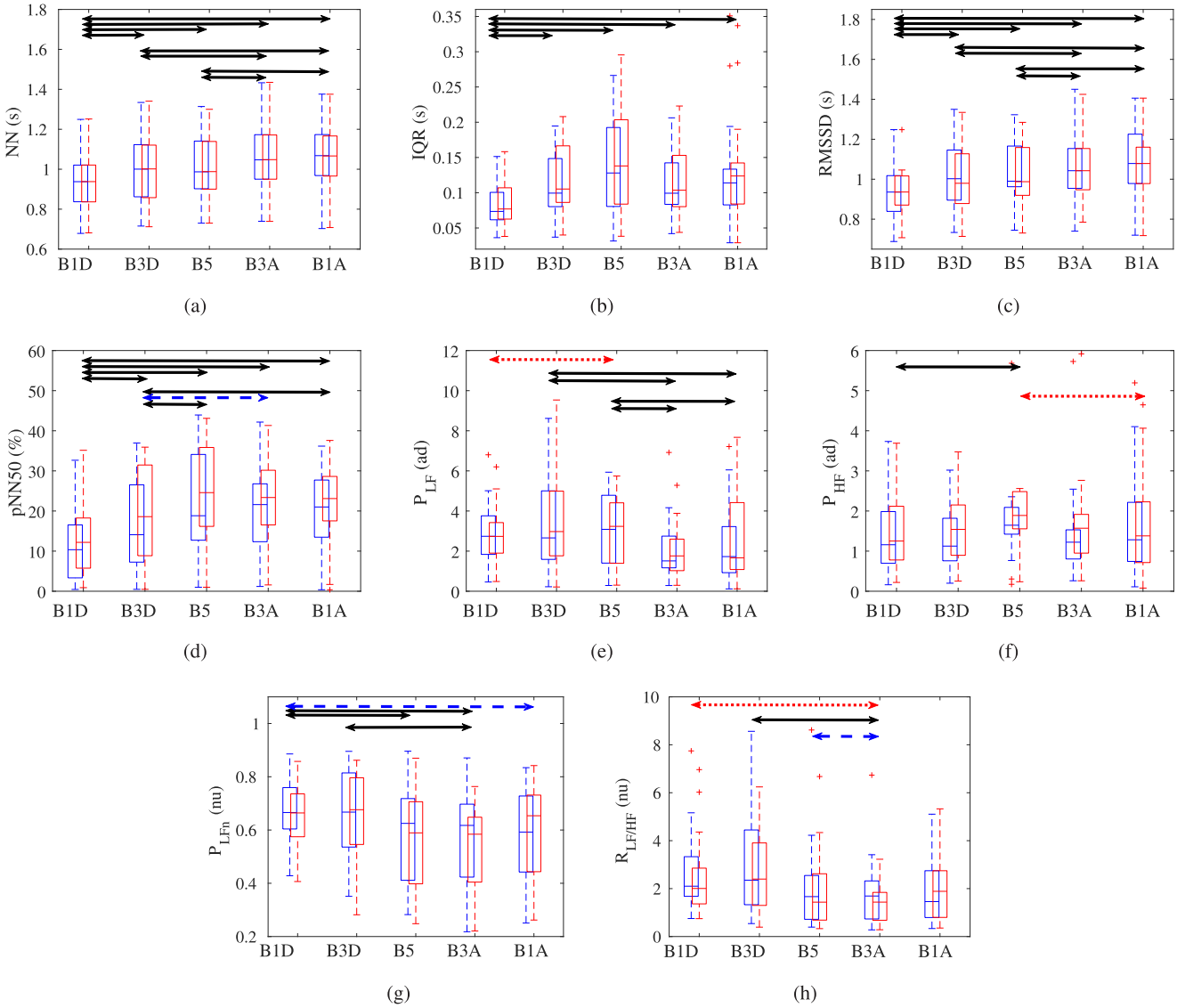

Fig. 5. Boxplots of the values shown in Table III. Blue plots represent ECG parameters and red ones PPG parameters. Significant differences between stages are represented by an arrow joining the two stages analysed (black arrow if differences are found in both ECG and PPG; blue dashed arrow when differences are only in ECG; red dotted arrow when only in PPG.)

To that end, the peakness criteria and thresholds were strictly imposed. For future applications in which only one signal is available (probably PPG), this respiratory rate estimation must change. One possible solution is to modify the peakness criteria and thresholds in order to be less restrictive and be able to estimate the respiratory rate over a longer period of time even though the respiratory information may be less clear. In summary, the parameters and algorithms could be modified depending on the final application.

The respiratory rate was used to complement the ANS information extracted from the HRV and PRV analysis, discarding those subjects with a respiratory rate lower than 0.15 Hz to avoid misinterpretations of the ANS response [20], [22], [23]. The first interesting point arising from our observations is that the ECG and PPG signals provide the same information. A similar behaviour has been reported previously [7]–[10], although there are no studies of the ECG and PPG at different atmospheric pressures. The results provided by ECG and PPG are very similar, as can be seen from Table III and Fig. 5. Although a difference between the ECG and PPG signals was observed, with power in high frequency band being higher when computed from the PPG, this behaviour has been reported in the literature [7]–[10]. Despite this minor difference, all the p-values comparing ECG and PPG parameters are higher than 0.05 and the correlation between features extracted from the ECG and PPG is very high (higher than 90% in almost all stages). These two results show that ECG and PPG signals provide the same information irrespective of atmospheric pressure.

Focusing now on the HRV and PRV results, the temporal parameters (NN, IQR, $RMSSD$ and $pNN50$) increase their value with respect to the first stage. These differences are significant, as shown in Fig. 5. Despite this common behaviour, two

different trends are observed: the increase in NN and $RMSSD$ values occurs during the entire test when comparing each stage with the previous one, whereas the increase in IQR and $pNN50$ ends at the deepest stage (B5). An increase in NN (and therefore decrease in heart rate) related to the time spent in a hyperbaric environment has been reported previously [24], [25], [27], [28]. This bradycardia could arise due to the fact that hyperoxia induces a peripheral vasoconstriction [45] or because the entry of chemoreceptors is reduced [46]. The behaviour observed for IQR and $pNN50$ could suggest that the vital signs of the subjects are more unstable at greater depths as these two parameters mostly reflect the stability of the signal. However, the IQR and $pNN50$ values in B3A and B1A are higher than in B3D and B1D, respectively, thus suggesting some degree of modification due to the time spent in the hyperbaric environment, as also seen from the significant differences between B5 and B3A vs. B3D. Note that, although not statistically significant differences exist some parameters change in opposite direction along hyperbaric variation trend. For instance IQR decreases from B5 to B3A but increases from B3A to B1A. As previously mentioned, this behaviour could be due to the long period of time spent in the decompression stops (44 min in almost all the subjects), but future studies are needed to corroborate this.

Each frequency parameter was evaluated individually. Thus, P_{LF} increased to a maximum for the deepest stage (B5), and then decreased quickly, reaching a minimum value for stages B3A and B1A. This pattern was found in both the ECG and PPG signals. Significant differences were found for B3A and B1A with respect to B3D and B5 because of this rapid decrease. A similar increase in LF power at higher atmospheric pressures has been reported in [29], but with no significant differences. The physiological interpretation of this parameter by itself is complicated as P_{LF} registers both sympathetic and parasympathetic responses, therefore no clear interpretation of when and why each ANS branch changes is possible. As such, it is better to analyse P_{HF} as a parasympathetic marker and P_{LF_n} and $R_{\text{LF/HF}}$ as sympathetic indices.

As mentioned above, a difference was observed between the ECG and PPG signals in P_{HF}, although this had no effect on the statistical analysis. Thus, this parameter increases until the highest pressure is reached, as seen in previous studies [24], [26], [27], [29]. Significant differences were only found in the deepest stage with respect to the initial stage (B5 vs. B1D) and in the final stage with respect to the deepest one (B1A vs. B5) for the PRV signal, thus reinforcing this pattern. A possible reason for this increase in P_{HF} could be the rise in peripheral vascular resistance that may occur in hyperbaric environments, which would cause a higher blood pressure leading to a baroreflex system reaction and so, an observation of an increase of the parasympathetic tone. A detailed study of the baroreflex system inside hyperbaric environments should be needed to confirm this hypothesis.

The sympathetic indices (P_{LF_n} and $R_{\text{LF/HF}}$) reach their maximum values in the first two stages (B1D and B3D) and then decrease, reaching a minimum in the final two stages (B3A and B1A). This normalised power decrease in the final stages when a considerable time is spent inside the chamber has been corroborated in other studies [24], [26], [27], [33]. The statistical differences in P_{LF_n} found for B5 and B3A vs. B1D, and for B3A vs. B3D, supports this theory.

To sum up the contribution of the frequency parameters, it should be noted that while the behaviour of the sympathetic components (P_{LF_n} and $R_{\text{LF/HF}}$) varies with the time spent inside the hyperbaric chamber, the parasympathetic component (P_{HF}) varies with changes in atmospheric pressure, which is one of the novel findings of this study. As P_{LF} registers the influence of both sympathetic and parasympathetic components, its behaviour does not show any clear pressure or time dependency. One possible explanation for this is that P_{LF} is affected by the time spent inside the chamber and by the pressure, thus meaning that its interpretation is difficult.

Finally, oxygen saturation remains stable during all stages due to the ventilation system of the hyperbaric chamber, which maintains a steady gas concentration. The possibility of being able to measure SpO_2 is very interesting, especially when subjects are exposed to compressed air, as in real diving. The percentage of oxygen in the body will allow hyperoxia to be identified and controlled, thus meaning that decompression stops can be performed based on this concentration instead of the time established in the tables. As such, use of the PPG signal in real diving would appear to be very useful, although further studies are required to analyse all the possibilities that this signal can provide in terms of subject analysis.

VI. Conclusion

It has been shown that the combined respiratory rate extracted from ECG and PPG signals increases in those stages when the atmospheric pressure is high and that the inclusion of respiratory information obtained from ECG and PPG signals helps to avoid misinterpretations in the ANS response. Furthermore, the temporal indices show that the beat-to-beat interval is higher in the last stages, thus meaning that the heart rate decreases with time spent in the chamber. The frequency domain HRV and PRV indices allow us to differentiate between the different stages, with HF power increasing with atmospheric pressure. This leads to a decrease in the sympathetic markers (P_{LF_n} and $R_{\text{LF/HF}}$) as more time is spent inside the chamber, thus allowing us to identify hyperbaric environments. In addition, it has been shown that the PRV signal provides a surrogate measurement of HRV in hyperbaric environments and, furthermore, the PPG signal provides very useful additional information such as the oxygen saturation, thus making the PPG signal a suitable tool in these situations.

Acknowledgment

The author would like to thank Hospital General de la Defensa de Zaragoza, that allowed to use the hyperbaric chamber; the assistance as volunteers of the Regimiento de Pontoneros y Especialidades de Ingenieros n^o12; and the support of the consolidated group BSICoS (Biomedical Signal Interpretation & Computational Simulation).

REFERENCES

[1] D. Z. Levett and I. L. Millar, "Bubble trouble: A review of diving physiology and disease," *Postgrad. Med. J.*, vol. 84, pp. 571–578, 2008.

[2] M. J Halsey, "Effects of high pressure on the central nervous system," *Physiol. J.*, vol. 62, pp. 1342–1377, 1982.

[3] E. P. Widmaier, H. Raff, and K. T. Strang, "Vander's Human Physiology. The Mechanisms of Body Function," 11 ed., Boston McGraw-Hill, 2008.

[4] M. Hagberg and H. Ornhagen, "Incidence and risk factors for symptoms of decompression sickness among male and female dive masters and instructors-a retrospective cohort study," *Undersea Hyperbar. M.*, vol. 30, no. 2, pp. 93–102, 2003.

[5] A. Pelliccia *et al.*, "Recommendations for competitive sports participation in athletes with cardiovascular disease: A consensus document from the Study Group of Sports Cardiology of the Working Group of Cardiac Rehabilitation and Exercise Physiology and the Working Group of Myocardial and Pericardial Diseases of the European Society of Cardiology," *Eur. Heart. J.*, vol. 26, pp. 1422–1445, 2005.

[6] M. Nitzan, A. Babchenko, B. Khanokh, and D. Landau, "The variability of the photoplethysmographic signal – a potential method for the evaluation of the autonomic nervous system," *Physiol. Meas.*, vol. 19, pp. 93–102, 1998.

[7] S. Lu *et al.*, "Can photoplethysmography variability serve as an alternative approach to obtain heart rate variability information?" *J. Clin. Monit. Comput.*, vol. 22, pp. 23–29, 2008.

[8] N. Selvaraj, A. K. Jaryal, J. Santhosh, K. K. Deepak, and S. Anand, "Assessment of heart rate variability derived from finger-tip photoplethysmography as compared to electrocardiography," *J. Med. Eng. Technol.*, vol. 32, pp. 479–484, 2008.

[9] K. Charlot, J. Cornolo, J. V. Brugniaux, J. P. Richalet, and A. Pichon, "Interchangeability between heart rate and photoplethysmography variabilities during sympathetic stimulations," *Physiol. Meas.*, vol. 30, pp. 1357–1369, 2009.

[10] E. Gil, M. Orini, R. Bailón, J. M. Vergara, L. Mainardi, and P. Laguna, "Photoplethysmography pulse rate variability as a surrogate measurement of heart rate variability during non-stationary conditions," *Physiol. Meas.*, vol. 31, pp. 1271–1290, 2010.

[11] I. Constant, D. Laude, I. Murat, and J. L. Elghozi, "Pulse rate variability is not a surrogate for heart rate variability," *Clin. Sci.*, vol. 97, pp. 391–397, 1999.

[12] Task Force of the European Society of Cardiology and the North American Society of Pacing and Electrophysiology, "Heart rate variability: Standards of measurement, physiological interpretation and clinical use," *Circulation*, vol. 93, pp. 1043–1065, 1996.

[13] G. B. Moody, R. G. Mark, A. Zoccola, and S. Mantero, "Derivation of respiratory signals from multi-lead ECGs," *Comput. Cardiol.*, vol. 12, pp. 113–116, 1986.

[14] B. Mazzanti, C. Lamberti, and J. de Bie, "Validation of an ECG-derived respiration monitoring method," *Comput. Cardiol.*, 2003, pp. 613–616.

[15] R. Bailón, L. Sornmo, and P. Laguna, "A robust method for ECG-based estimation of the respiratory frequency during stress testing," *IEEE Trans. Biomed. Eng.*, vol. 53, no. 7, pp. 1273–1285, Jul. 2006.

[16] J. Lázaro, A. Alcaine, D. Romero, E. Gil, P. Laguna, E. Pueyo, and R. Bailón, "Electrocardiogram derived respiratory rate from QRS slopes and R-Wave angle," *Ann. Biomed. Eng.*, vol. 40, no. 10, pp. 2072–2083, 2014.

[17] K. H. Chon, S. Dash, and K. Ju, "Estimation of respiratory rate from photoplethysmogram data using time-frequency spectral estimation," *IEEE Trans. Biomed. Eng.*, vol. 56, no. 8, pp. 2054–2063, Aug. 2009.

[18] J. Lázaro, E. Gil, R. Bailón, A. Mincholé, and P. Laguna, "Deriving respiration from photoplethysmographic pulse width," *Med. Biol. Eng. Comput.*, vol. 51, pp. 233–242, 2013.

[19] P. H. Charlton *et al.*, "Breathing rate estimation from the electrocardiogram and photoplethysmogram: A review," *IEEE Reviews Biomed. Eng.*, vol. PP, no. 99, pp. 1–17, 2017.

[20] P. Z. Zhang, W. N. Tapp, S. S. Reisman, and B. H. Natelson, "Respiration response curve analysis of heart rate variability," *IEEE Trans. Biomed. Eng.*, vol. 44, no. 4, pp. 321–325, Apr. 1997.

[21] R. Bailón, L. Mainardi, M. Orini, L. Srnmo, and P. Laguna, "Analysis of heart rate variability during exercise stress testing using respiratory information," *Biomed. Signal Process. Control*, vol. 5, pp. 299–310, 2010.

[22] X. Long, P. Fonseca, R. Haakma, R. M. Aarts, and J. Foussier, "Spectral boundary adaptation on heart rate variability for sleep and wake classification," *Int. J. Artif. Intell. Tools*, vol. 23, pp. 01–20, 2014.

[23] A. Hernando *et al.*, "Inclusion of respiratory frequency information in heart rate variability analysis for stress assessment," *IEEE J. Biomed. Health Inform*, vol. 20, no. 4, pp. 1016–1025, Jul. 2016.

[24] V. Lund, J. Laine, T. Laitio, E. Kentala, J. Jalonen, and H. Scheinin, "Instantaneous beat-to-beat variability reflects vagal tone during hyperbaric hyperoxia," *Undersea Hyperbar. M.*, vol. 30, pp. 29–36, 2003.

[25] K. Yamauchi, Y. Tsutsui, Y. Endo, S. Sagawa, F. Yamazaki, and K. Shiraki, "Sympathetic nervous and hemodynamic responses to lower body negative pressure in hyperbaria in men," *Amer. J. Physiol. Regulatory Integrative Comparative Physiol.*, vol. 282, pp. R38–45, 2002.

[26] V. Lund *et al.*, "Heart rate variability in healthy volunteers during normobaric and hyperbaric hyperoxia," *Acta Physiol. Scand.*, vol. 167, pp. 29–35, 1999.

[27] E. Barbosa *et al.*, "Effect of Hyperbaric Pressure During scuba diving on autonomic modulation of the cardiac response: Application of the continuous wavelet transform to the analysis of heart rate variability," *Mil. Med.*, vol. 175, no. 1, pp. 61–64, 2010.

[28] D. R. Seals, D. G. Johnson, and R. F. Fregosi, "Hyperoxia lowers sympathetic activity at rest but not during exercise in humans," *Amer. J. Physiol.*, vol. 260, pp. R873–R878, 1991.

[29] V. Lund, E. Kentala, H. Scheinin, J. Klossner, K. Sariola-Heinonen, and J. Jalonen, "Hyperbaric oxygen increases parasympathetic activity in professional divers," *Acta Physiol. Scand.*, vol. 170, pp. 39–44, 2000.

[30] H. Al-Haddad, P. B. Laursen, D. Chollet, F. Lemaitre, S. Ahmaidi, and M. Buchheit, "Effect of cold or thermoneutral water immersion on post-exercise heart rate recovery and heart rate variability indices," *Auton. Neurosci.*, vol. 156, no. 1/2, pp. 111–116, 2010.

[31] R. Perini and A. Veicsteinas, "Heart rate variability and autonomic activity at rest and during exercise in various physiological conditions," *Eur. J. Appl. Physiol. Occup. Physio.*, vol. 90, no. 3/4, pp. 317–325, 2003.

[32] J. D. Schipke and M. Pelzer, "Effect of immersion, submersion, and scuba diving on heart rate variability," *Brit. J. Sports Med.*, vol. 35, pp. 174–180, 2001.

[33] F. Chouchou, V. Pichot, M. Garet, J. C. Barthelemy, and F. Roche, "Dominance in cardiac parasympathetic activity during real recreational scuba diving," *Eur. J. Appl. Physiol.*, vol. 106, pp. 345–352, 2009.

[34] L. M. Ueno *et al.*, "Effect of aging on carotid artery stiffness and baroreflex sensitivity during head-out water immersion in man," *Braz J. Med. Biol. Res.*, vol. 38, no. 4, pp. 629–637, 2005.

[35] D. Sokas, M. Gailius, and V. Marozas, "Diver physiology monitor and its graphical user interface," *Virt. Inst. Biomed.*, vol. 2, pp. 5–9, 2016.

[36] L. Sornmo and P. Laguna, "Bioelectrical signal processing in cardiac and neurological applications," Amsterdam, The Netherlands: Elsevier, 2005.

[37] J. P. Martínez, R. Almeida, S. Olmos, A. P. Rocha, and P. Laguna, "A wavelet-based ECG delineator: Evaluation on standard databases," *IEEE Trans. Biomed. Eng.*, vol. 51, no. 4, pp. 570–581, Apr. 2004.

[38] J. Mateo and P. Laguna, "Analysis of heart rate variability in the presence of ectopic beats using the heart timing signal," *IEEE Trans. Biomed. Eng.*, vol. 50, no. 3, pp. 334–343, Mar. 2003.

[39] E. Gil, J. M. Vergara, and P. Laguna, "Detection of decreases in the amplitude fluctuation of pulse photoplethysmography signal as indication of obstructive sleep apnea syndrome in children," *Biomed. Signal Process. Control*, vol. 3, no. 3, pp. 267–277, 2008.

[40] J. Lázaro, E. Gil, J. M. Vergara, and P. Laguna, "Pulse rate variability analysis for discrimination of sleep-apnea-related decreases in the amplitude fluctuations of PPG signal in children," *IEEE J. Biomed. Health Inform.*, vol. 18, no. 1, pp. 240–246, Jan. 2014.

[41] J. Y. A. Foo and C. S. Lim, "Pulse transit time as an indirect marker for variations in cardiovascular related reactivity," *Technol. Health Care*, vol. 14, pp. 97–108, 2006.

[42] R. Bailón, G. Laouini, C. Grao, M. Orini, P. Laguna, and O. Meste, "The integral pulse frequency modulation with time-varying threshold: Application to heart rate variability analysis during exercise stress testing," *IEEE Trans. Biomed. Eng.*, vol. 58, no. 3, pp. 642–652, Mar. 2011.

[43] E. Pueyo, L. Sornmo, and P. Laguna, "QRS slopes for detection and characterization of myocardial ischemia," *IEEE Trans. Biomed. Eng.*, vol. 55, no. 2, pp. 468–477, Feb. 2008.

[44] A. V. Challoner, "Photoelectric plethysmography for estimating cutaneous blood flow," *Non-Inv. Physiol. Meas.*, vol. 1, pp. 125–151, 1979.

[45] W. M. Panneton, "The mammalian diving response: An enigmatic reflex to preserve life?" *Physiol.*, vol. 28, no. 5, pp. 284–297, 2013.

[46] J. M. Marshall, "Chemoreceptors and cardiovascular control in acute and chronic systemic hypoxia," *Braz. J. Med. Biol. Res.*, vol. 31, no. 7, pp. 863–888, 1998.